TRANSPORT PHENOMENA OF CROSSFLOW OVER CIRCULAR CYLINDER WITH SECONDARY JET

M. Yaman, M. ABO EL-NASR, W. Aboelsoud[1]

Mechanical Power Engineering, Ain Shams University, Cairo, 11517, Egypt

Abstract

Enhancement of the convective heat transfer on air side is a challenging problem due to the poor thermal characteristics of air as well as the high thermal resistance caused by the boundary layer. There are many ways to enhance thermal convection like using extended surface and porous media. An innovative method to improve the convective heat transfer of cross air flow over a circular cylinder by the application of secondary air jet is introduced in this study to suppress the boundary layer and thus reduce thermal resistance. A two-dimensional numerical model is developed which consists of a hollow circular cylinder made of copper, with a 5 cm outside diameter and 1 cm inside diameter. The cylinder is in the middle of an air channel 2 m long. A heat flux of 6.6 W/cm^2 is applied on the inner boundary of the cylinder. A secondary air jet was applied, from a 5 mm slit on the upper wall of the air channel, with different angles (theta) of 25 to 155 degrees. The position of the air jet also varied from above the stagnation point to other positions downstream (S). This distance of the applied jet relative to the diameter of the cylinder (S/D) varied from 0 to 1.2. The height of the air channel relative to the diameter of the cylinder (H/D) was changed from 2 to 8. At constant H/D, the total mass flow rate is kept constant in both cases, with and without the jet having the same channel height. After validation, a comparison between the average Nusselt number in all cases and the case where there is no air jet was carried out. Results show that there is an enhancement of the average heat transfer coefficient of up to six times the case with no jet.

Keywords: Crossflow heat exchanger – Jet cooling – Boundary layer suppression

[1] Corresponding Author: walid.aboelsoud@eng.asu.edu.eg

Nomenclature

Nu	Nusselt number
Re	Reynolds number
Pr	Prandtl number
S	the position of the air jet from above the stagnation point to other positions downstream
D	The outer diameter of the cylinder
d_i	The inner diameter of the cylinder
S/D	The distance of the applied jet relative to the diameter of the cylinder
H/D	The height of the air channel relative to the diameter of the cylinder
q``	The heat flux applied on the inner wall of the cylinder
k	Thermal conductivity of air
T_s	The average surface temperature of the cylinder
T_a	The bulk air inlet temperature
$\overline{Nu}$	The average Nusselt number for the case of crossflow without jet
$\overline{Nu_j}$	The average Nusselt number for the case of crossflow with secondary air jet
θ	The secondary jet inclination angle

1. INTRODUCTION

Air cooling of a circular cylinder is of great importance due to the large number of applications it is associated with. There have been many studies on the cooling of a cylinder to achieve improve the heat transfer mechanism. Heat transfer enhancement can be accomplished in many ways like using an extended surface or porous media.

Singh et al [1] carried out experimental and numerical studies on the cooling of a heated circular cylinder using double circular jet of air to examine flow and heat transfer characteristics maintaining the surface of the cylinder at iso-flux boundary condition. The study examined the effect of flow confinement using semi-circular flow below the heated cylinder on heat transfer. Reynolds number, Re_d defined based on the diameter of the nozzle, the non-dimensional distance between double the jets (s/d), and the ratio of the non-dimensional distance between the nozzle exit and the circular cylinder surface (h/d) ranged from 10,000 to 25,000, 4–20 and 4–16, respectively in the study while the ratio of the diameter of the nozzle to the diameter of the heated cylinder, d/D was kept constant at 0.208. Results showed that there is no appreciable change in Nusselt number of the stagnation point at s/d, however, the average Nusselt number over the cylinder surface increases by increasing s/d. Both experimental and numerical results showed that confinement at the bottom of the cylinder enhanced the heat transfer. The average Nusselt number increases

using the confinement by about 16% at h/d = 16 but only by 10% at h/d = 4 for the same Re_d.

Singh et al. [2] performed an experimental and numerical study on the cooling of a circular cylinder using a circular air jet with constant heat flux. A study was carried out to understand the effect of flow confinement on hydraulic and thermal performance. The parameters under investigation were the radius of the condiment, Reynolds number of the jet. Four different values of the nozzle-to-cylinder distance were considered. The distribution of the local Nusselt number was obtained from the experiment. While flow and temperature fields were obtained from the numerical model. Results showed an improvement in local Nusselt number by 24% and 17% in average Nusselt number. Numerical studies were also carried out with semi-circular flow confinement with an opening at the bottom. This configuration was found to result in a maximum increase in the local Nusselt number by 24% compared to the results with confinement without an opening. It was found in all the cases considered that the percentage increase in the average Nusselt number due to the confinement was higher at Re_d = 10,000 than that at Re_d = 25,000. Also, there was a significant reduction in the highest temperature at the cylinder ends using flow confinement. It was shown numerically that the local heat transfer increased by 24% in the center portion of the cylinder using confinement with a bottom opening.

Singh et al. [3] examined the cooling of a circular heated cylinder using turbulent circular air jet impingement experimentally and numerically. The examination was obtained by maintaining constant heat flux at the surface of the heated cylinder with varying Reynolds number, Re_d defined based on the nozzle diameter, from 10,000 to 25,000. The non-dimensional distance between the nozzle exit and the circular cylinder, h/d, and the ratio of nozzle diameter to the diameter of the heated target cylinder, d/D, were considered as geometric parameters in the range of 4–16 and 0.11–0.25, respectively. A numerical investigation was performed to study the flow features and to attain the temperature and local Nusselt number distributions over the surface of the heated cylinder. The results showed that as the h/d decreases the stagnation Nusselt number increases monotonically and that h/d and d/D have a significant effect on the jet impinging region only. A correlation for Nusselt number at the stagnation point was developed based on the experimental results with a good agreement.

Bharti et al. [4] carried out numerical studies using a finite volume method (FVM) on a Cartesian grid system for forced convection heat transfer from an unconfined circular cylinder in the steady crossflow regime where Reynolds number (Re) varied from 10 to 45 and Prandtl number (Pr) varied from 0.7 to 400 to develop simple correlations for Nusselt number. The examination considered the effects of Re, Pr, thermal boundary conditions, and the temperature field near the cylinder on the local Nusselt number distributions to understand the nature of the flow. The results prevailed that the rate of heat transfer increases by increasing Reynolds numbers and/or Prandtl numbers. The isoflux condition always shows a higher heat transfer coefficient than the isothermal condition at the surface of the cylinder for the same Reynolds and Prandtl numbers with maximum difference between the two values of about 15–20.

Mettu et al. [5] carried out a numerical investigation using FLUENT to study the unsteady momentum and heat transfer from an asymmetrically confined circular cylinder in a plane channel with Reynolds numbers range of $10 < Re < 500$, blockage ratio of $0.1 < \beta < 0.4$, and gap ratio of $0.125 < \gamma < 1$ maintaining Prandtl number at 0.744. The flow transition from steady to unsteady (characterized by critical Re) was obtained as a function of γ and β. The numerical investigation was performed to study the effect of γ on the mean drag (C_D) and lift (C_L) coefficients, Strouhal number (St), and Nusselt number (Nu_w). It was noticed that the critical Reynolds number increases as γ decreases for all values of β, while as γ decreases (C_D) and (St) increase for fixed values of β and Re. It was found that decreasing γ has a negligible effect on Nu_w for all the blockage ratios examined.

W. A. Khan et al. [6] employed an integral approach of the boundary layer analysis to investigate fluid flow and heat transfer characteristics for flow around an infinite circular cylinder. The study used Von Karman–Pohlhausen method to solve momentum integral equation and the energy integral equation for both isothermal and isoflux boundary conditions. The fourth-order velocity profile in the hydrodynamic boundary layer and the third-order temperature profile inside the thermal boundary layer were used to solve the momentum integral and the energy integral equations, respectively. The investigation obtained closed-form expressions for the drag and the average heat transfer coefficients for a board range of Reynolds and Prandtl numbers. It was found that there was a good agreement for the approach with the

experimental results for the full laminar range of Reynolds numbers without stream turbulence and blockage effects.

W. A. Khan et al. [7] investigated the effects of blockage on fluid flow and heat transfer from a circular cylinder confined between parallel planes. For isothermal and isoflux boundary conditions, the fourth-order velocity profile in the hydrodynamic boundary layer and the third-order temperature profile inside the thermal boundary layer were used to solve the momentum integral and the energy integral equations, respectively. Image processing was used to obtain the potential flow velocity outside the boundary layer. The parameters used to obtain the closed-form solutions were the blockage ratio, Reynolds, and Prandtl numbers. It was noticed that the blockage ratio dominates the fluid flow and the transfer of heat from the cylinder and postpones the separation.

Correlations were obtained to determine the drag coefficient and the dimensionless heat transfer coefficient from a cylinder confined in a channel at different blockage ratios. There was a good agreement between the experimental and numerical results for a broad range of blockage ratios, Reynolds numbers, and Prandtl numbers.

S. Sanitjai et al. [8] investigated the local and average heat transfer from a circular cylinder by forced convection for Reynolds number range of 2,000 to 90,000 and Prandtl number of 0.7 to 176. It was found that Nusselt number strongly depends on the Reynolds number and the Prandtl number with different power indices in each region for subcritical flow where there are three regions of flow around the cylinder: laminar boundary layer region, reattachment of shear layer region, and periodic vortex flow region. Also, the average heat transfer was calculated and correlated with the Reynolds number and the Prandtl number in each region. An empirical correlation for predicting the overall heat transfer from the cylinder was developed from the contributions of heat transfer in these regions.

A. A. Tawfek [9] performed an experimental study of heat transfer characteristics of a circular jet impinging on a cylinder at isothermal boundary condition. Reynolds number Re_d varied from 3800 to 40,000, h/d = 7–30 and d/D = 0.06–0.14. It was shown that the Nusselt number decreases monotonically along the axial and circumferential directions. Also, a correlation was presented for Nusselt number at the stagnation point based on the experimental results. **A. A. Tawfek. [10]** examined the heat transfer due

to an inclined circular jet impinging on a constant temperature circular cylinder.

In the present study, the convective heat transfer of cross airflow over a circular cylinder by the application of secondary air jet is studied numerically. The novelty of this work is to target the suppression of the boundary layer by introducing a secondary jet flow of air. For comparison purposes, Thermal performance with the total mass flow rate from the air jet and the crossflow of air combined will be compared to that of no jet having the same mass flow rate of air from the crossflow of air only. The jet was applied to the main cross airflow with different angles (θ) at different duct heights (H) and jet positions (S).

2. METHODOLOGY

2.1 Model

The geometry of the numerical model under study is shown in **Figure 1**. It consists of a two-dimensional air duct 1600 mm long with a variable height of 100 mm to 800 mm. A hollow circular cylinder with an outside diameter of 50 mm and an inside diameter of 40 mm, is placed in the middle of the air duct. A secondary air jet is generated on the top surface of the air duct with variable position and angle. The air jet penetrates the main flow from an opening slit of 5 mm. The position of the secondary jet starts from a point just above the stagnation point on the cylinder surface and progresses downstream. So the jet position (S) is measured from the starting point and equals 0, 10, 20, 30, 40, and 50 mm. The jet angle varies from 15 ^{o} to 165^{o} with 15^{o} increments. The main flow of air is applied with an inlet velocity of 1 m/s, while the secondary air is generated with a velocity of 16 m/s.

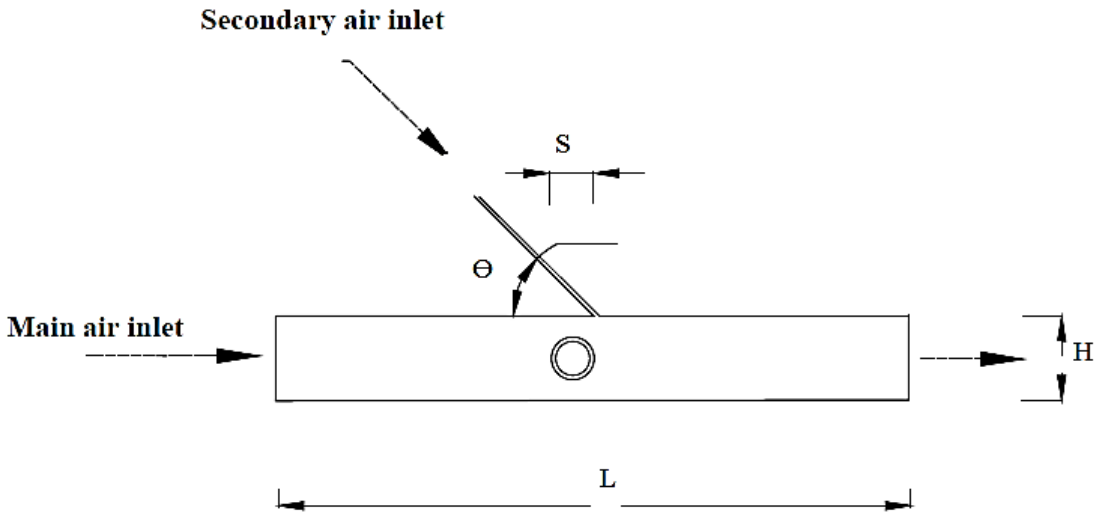

Figure 1 The geometry of the numerical model

2.2 Governing equations

The computational domain consists of two domains (The first domain is copper while the second domain is air). In the present study, COMSOL Multiphysics software is used to solve velocity, pressure, and temperature fields using the finite element method (FEM). The governing equations are as follows:

- Continuity Equation

Air flows steadily under turbulent conditions in the first computational domain. The air density depends on temperature and pressure. The variation of density is considered taking into consideration their variation with the position (x, y). The continuity equation would be:

$$\nabla.(\rho \mathbf{u}) = \mathbf{0} \qquad 1$$

- Momentum Equation

The dynamic viscosity of air is a function of its temperature which changes with the position, the airflow is turbulent then the momentum equation is:

$$\boldsymbol{\rho}\,(\mathbf{u}.\boldsymbol{\nabla})\,\mathbf{u} = \boldsymbol{\nabla}.\left[-\boldsymbol{\rho}\mathbf{I} + (\mu+\mu_{\mathbf{T}})\left(\boldsymbol{\nabla}\mathbf{u} + (\boldsymbol{\nabla}\mathbf{u}^{\mathbf{T}})\right) - \frac{\mathbf{2}}{\mathbf{3}}\,(\mu+\mu_{\mathbf{T}})(\boldsymbol{\nabla}.\mathbf{u})\mathbf{I} - \frac{\mathbf{2}}{\mathbf{3}}\,\boldsymbol{\rho}\mathbf{k}\mathbf{I}\right] + \mathbf{F} \quad \mathbf{2}$$

$$\boldsymbol{\rho}\,(\mathbf{u}.\boldsymbol{\nabla})\,\mathbf{k} = \boldsymbol{\nabla}.\left[\left(\mu + \frac{\mu_{\mathbf{T}}}{\boldsymbol{\sigma}_{\mathbf{k}}}\right)(\boldsymbol{\nabla}\mathbf{k})\right] + \mathbf{P}_{\mathbf{k}} - \boldsymbol{\rho}\boldsymbol{\varepsilon} \quad \mathbf{3}$$

$$\boldsymbol{\rho}\,(\mathbf{u}.\boldsymbol{\nabla})\,\boldsymbol{\varepsilon} = \boldsymbol{\nabla}.\left[\left(\mu + \frac{\mu_{\mathbf{T}}}{\boldsymbol{\sigma}_{\boldsymbol{\varepsilon}}}\right)(\boldsymbol{\nabla}\boldsymbol{\varepsilon})\right] + \mathbf{C}_{\boldsymbol{\varepsilon}\mathbf{1}}\frac{\boldsymbol{\varepsilon}}{\mathbf{k}}\mathbf{P}_{\mathbf{k}} - \mathbf{C}_{\boldsymbol{\varepsilon}\mathbf{2}}\boldsymbol{\rho}\frac{\boldsymbol{\varepsilon}^{\mathbf{2}}}{\mathbf{k}} \quad \mathbf{4}$$

$$\mu_{\mathbf{T}} = \boldsymbol{\rho}\mathbf{C}_{\mu}\frac{\mathbf{k}^{\mathbf{2}}}{\boldsymbol{\varepsilon}} \quad \mathbf{5}$$

$$\mathbf{P}_{\mathbf{k}} = \mu_{\mathbf{T}}\left[\boldsymbol{\nabla}\mathbf{u}:\left(\boldsymbol{\nabla}\mathbf{u} + (\boldsymbol{\nabla}\mathbf{u}^{\mathbf{T}})\right) - \frac{\mathbf{2}}{\mathbf{3}}\,(\boldsymbol{\nabla}.\mathbf{u})^{\mathbf{2}}\right] - \frac{\mathbf{2}}{\mathbf{3}}\,\boldsymbol{\rho}\mathbf{k}\boldsymbol{\nabla}.\mathbf{u} \quad \mathbf{6}$$

$$\boldsymbol{\varepsilon} = \mathbf{e}\mathbf{P} \quad \mathbf{7}$$

$C_{\varepsilon 1}$	$C_{\varepsilon 2}$	C_{μ}	σ_k	σ_{ε}
1.44	1.92	0.09	1	1.3

- Energy Equation

In the present analysis, the variation in air thermal conductivity due to temperature change has been considered. With the assumption that the viscous dissipation term is neglected, the energy equation is:

$$\mathbf{d}_{\mathbf{z}}\boldsymbol{\rho}\mathbf{C}_{\mathbf{P}}\mathbf{u}.\boldsymbol{\nabla}\mathbf{T} = \boldsymbol{\nabla}.(\mathbf{d}_{\mathbf{z}}\mathbf{k}\boldsymbol{\nabla}\mathbf{T}) + \mathbf{d}_{\mathbf{z}}\mathbf{Q} + \mathbf{Q}_{\mathbf{vd}} + \mathbf{Q}_{\mathbf{p}} + \mathbf{Q}_{\mathbf{oop}} \quad \mathbf{8}$$

2.3 Boundary conditions

A crossflow of air enters the computational domain with uniform velocity and temperature. An air jet is introduced to the crossflow from the top of the computational domain with a velocity that is 16 times that of the crossflow at the same temperature. The top and bottom boundaries are thermally insulated while the inlet boundaries are at a temperature of 293 K. **Figure 2** show the boundaries of the numerical model. The inner surface of the copper cylinder supplies a constant heat flux of 6.6 W/cm^2. **Table 1** shows the hydrodynamic and thermal boundary conditions.

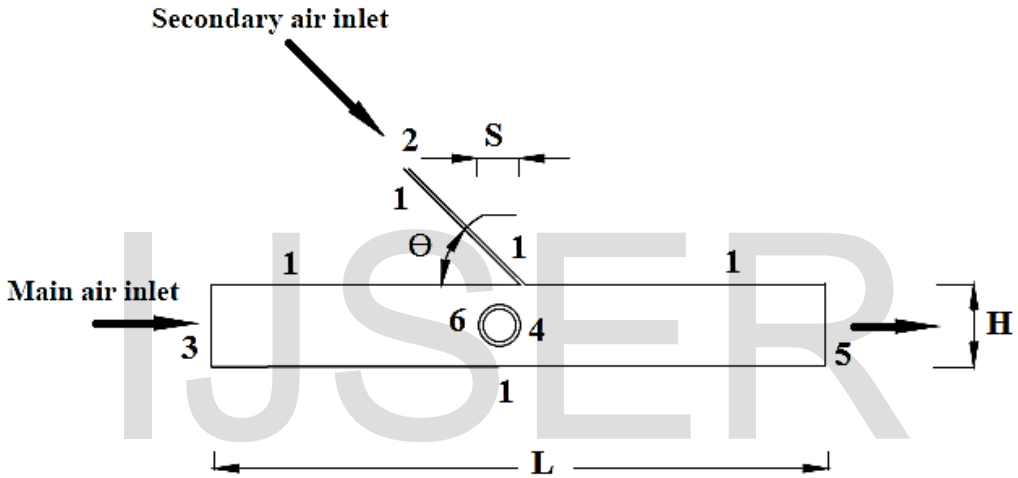

Figure 2 The boundaries of the numerical model

Table 1 Hydrodynamic and thermal boundary conditions

Boundary	Thermal boundary Conditions			Hydrodynamic boundary Conditions		
	Condition	Parameter	Units	Condition	Parameter	Units
1	Thermal insulation	$\partial T/\partial y$	0	No Slip	Velocity	0
2	Inlet	Temperature	293 K	Inlet	Velocity	16 m/s
3	Inlet	Temperature	293 K	Inlet	Velocity	1 m/s
4	----------	----------	---------	No Slip	Velocity	0
5	Outlet (symmetry)	$\partial T/\partial x$	0	Outlet	pressure	0
6	Constant heat flux	Heat flux (q")	6.6 W/cm^2	No Slip	Velocity	0

2.4 Dependency Study:

Mesh and Domain dependency tests are crucial in numerical analysis. These tests provide the information of the grid and domain sizes required to introduce an accurate, consistent, yet stable model.

2.4.1 Mesh Dependency Test:

The mesh dependency test was performed by making three tests at different (H/D) values. For each test, the average surface temperature of the cylinder (T_s) was determined by varying the number of elements in the selected mesh as shown in Figure 3. It was observed from the results shown below that the average surface temperature varied by choosing finer mesh. **Figure 3** shows that after about 2,000,000 element the surface temperature becomes constant without any significant change.

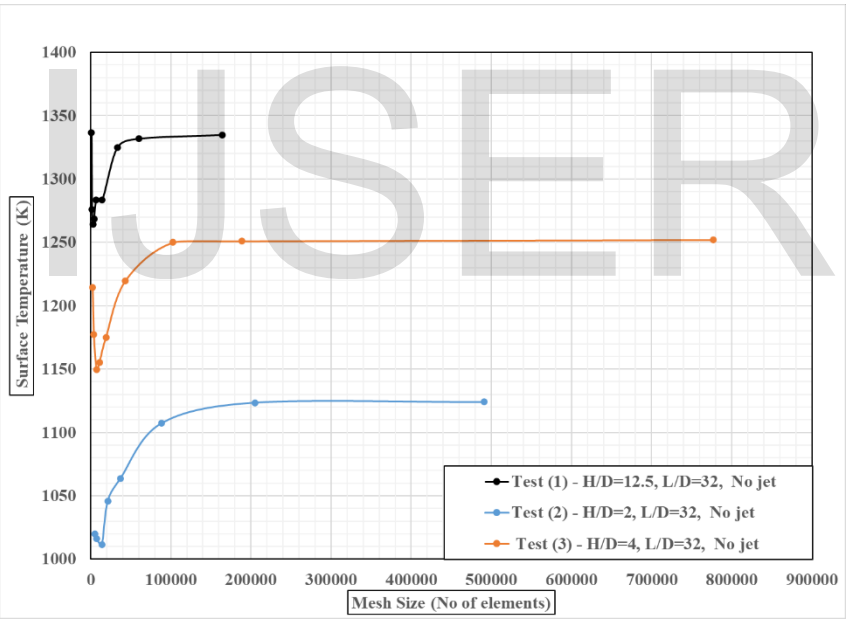

Figure 3 Mesh Dependency Test.

2.4.2 Domain Dependency Test:

Also, the domain dependency test was examined by varying the duct length and studying its effect on the average surface temperature of the cylinder as shown in **Figure 4**. From the results obtained, the suitable duct length of 40D was chosen.

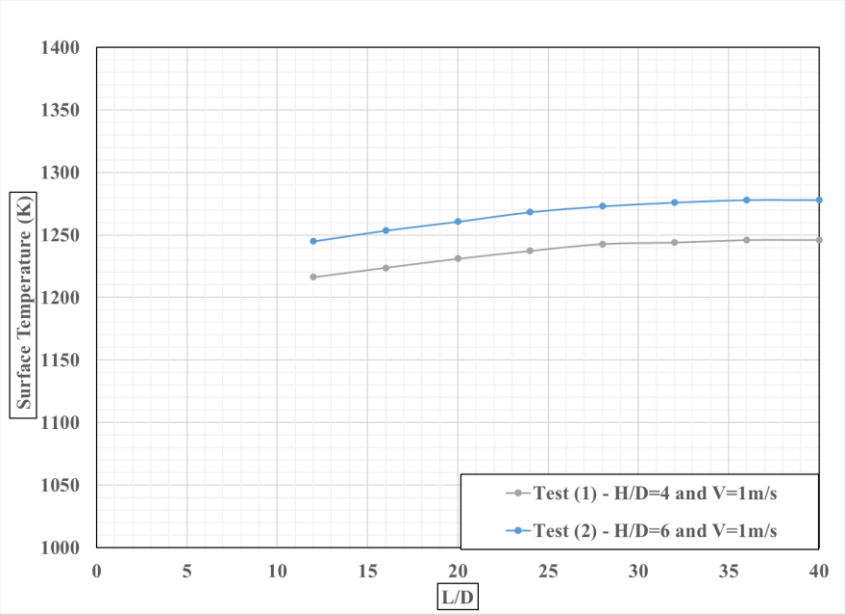

Figure 4 Domain Dependency Test.

2.5 MODEL VALIDATION:

Numerical data of crossflow of air over a circular cylinder was obtained and compared to **R.M. Fand [11]** for validation, **equation (9)**. **Figure 3** shows the relationship between Nusselt number and Reynolds number for the present model and Fand`s work. In the present model, The average Nusselt number is calculated from **equation (10)** .

$$\mathbf{Nu} = \left(\mathbf{0.35 + 0.34 * Re^{0.5} + 0.15 * Re^{0.58}}\right)\mathbf{Pr^{0.3}} \quad \textbf{9}$$

$$\overline{\mathbf{Nu}} = \frac{\mathbf{q`` * d_i}}{\mathbf{k * (T_s - T_a)}} \quad \textbf{10}$$

Where;

- q`` : the heat flux applied on the inner wall of the cylinder
- d_i : the inner diameter of the cylinder
- k : the thermal conductivity of air
- T_s : the average surface temperature of the cylinder
- T_a : the bulk inlet air temperature

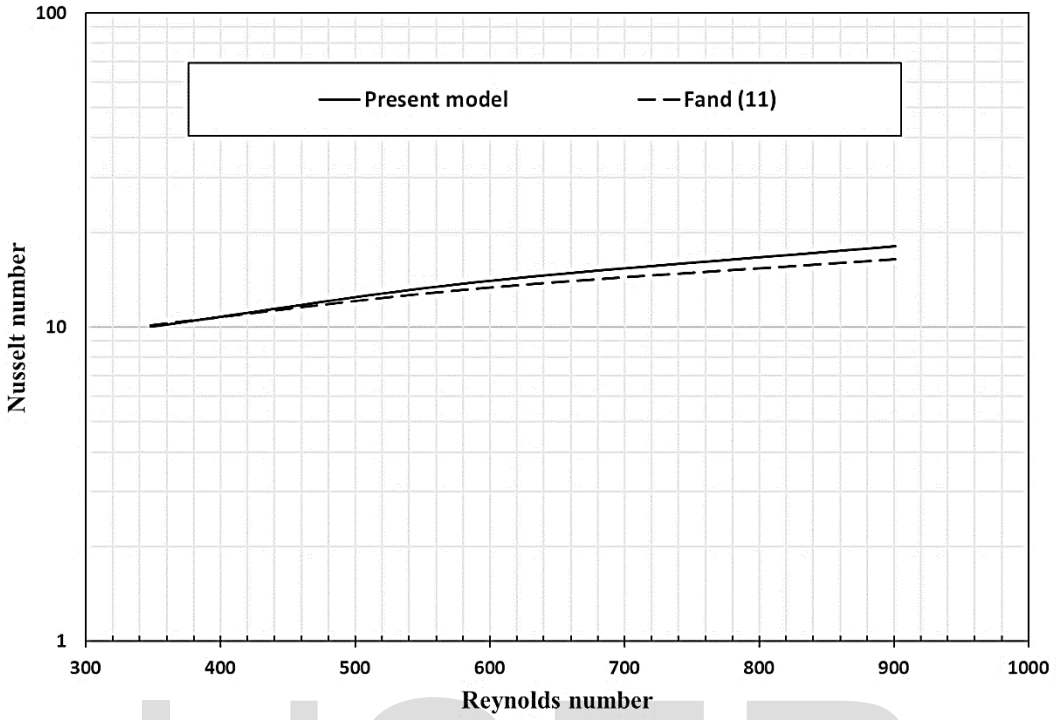

Figure 3 Validation of the numerical model.

3. RESULTS AND DISCUSSION

In the present study, the convective heat transfer of cross air flow over a circular cylinder by the application of secondary air jet is investigated numerically. Nusselt number is obtained at different values for S/D, H/D, and θ. Results show a dramatic enhancement of the heat transfer coefficient due to the suppression of the boundary layer by the secondary air jet.

Figure 6 shows the relationship between the average Nusselt number ratio ($\overline{Nu}_J/\overline{Nu}$), Nusselt number with the jet to that without the jet having the same total mass flow rate of air, and the inclination angles of the jet θ at H/D = 2 and S/D of 0, 0.2, 0.5, 0.7, 1, and 1.2. Results show that there is no effect of the jet on Nusselt number from an angle (θ) of 25° to 40°. Nusselt number starts to steeply increase from 40° to 155° based on the position of the secondary jet. It peaks out at different angles for each position with nearly the same value of about 5.5 times the case with no jet.

Figure 6 also shows that increasing the inclination angle of the jet (θ) from 25° to 90° at S/D=0 increases $\overline{Nu_j}/\overline{Nu}$ from about 1 to 5.2 while at S/D=0.2 $\overline{Nu_j}/\overline{Nu}$ increases to 4.8 at θ = 90°. On the other hand, increasing the inclination angle of the jet (θ) from 25° to 125° at S/D=0.5 increases $\overline{Nu_j}/\overline{Nu}$ to 5.4 while at S/D=0.7 $\overline{Nu_j}/\overline{Nu}$ reaches 5.2 at θ = 135°.

It is also observed that as the inclination angle of the jet (θ) increases, $\overline{Nu_j}/\overline{Nu}$ reaches its maximum value at different inclination angles for different jet positions S/D at H/D=2. Also, it is concluded that there is an enhancement of the average heat transfer coefficient of up to 5.4 times the case with no jet. As the position of the jet start to progress downstream (S/D = 1 and 1.2), the enhancement of Nusselt number starts to decay and this is attributed to the limitation of the jet momentum reaching the surface of the cylinder. At S/D = 1 and 1.2, there is almost no enhancement in Nusselt number up to θ = 120° then when the jet start to be directed upstream, its momentum has the chance to reach the surface of the cylinder and Nusselt number ratio starts to rise up to 4.6

Figure 7 shows the velocity field for H/D = 2, S/D = 0.5, and θ = 125°. It shows that although the inclination angle is 125° the effective angle is approximately 90° and this is attributed to the crossflow effect when merged with the jet. The overall effect magnifies when the effective impingement angle is ~ 90°. The flow around the cylinder is divided into two parts one downstream and the second upstream. The downstream flow generates higher velocity around the cylinder surface while its counterpart produces lower velocity but higher turbulence. With such perturbation from the jet momentum normal to the surface of the cylinder, suppression of the boundary layer is a fact that can be seen from the enhancement in $\overline{Nu_j}/\overline{Nu}$ as shown in **Figure 6**.

Figure 8 shows the relationship between $\overline{Nu_j}/\overline{Nu}$ and the jet angle (θ) at H/D = 4 and different jet positions. Increasing the jet angle (θ) from 25° to 115° at S/D = 0 increases $\overline{Nu_j}/\overline{Nu}$ from about 1 to 5.4 while at S/D = 0.2 $\overline{Nu_j}/\overline{Nu}$ reaches 5.6 at θ = 115°. On the other hand, at S/D = 0.5 Nuj/Nu reaches 5.6 at θ = 125° while at S/D=0.7 $\overline{Nu_j}/\overline{Nu}$ is 5.8 at θ = 135°.

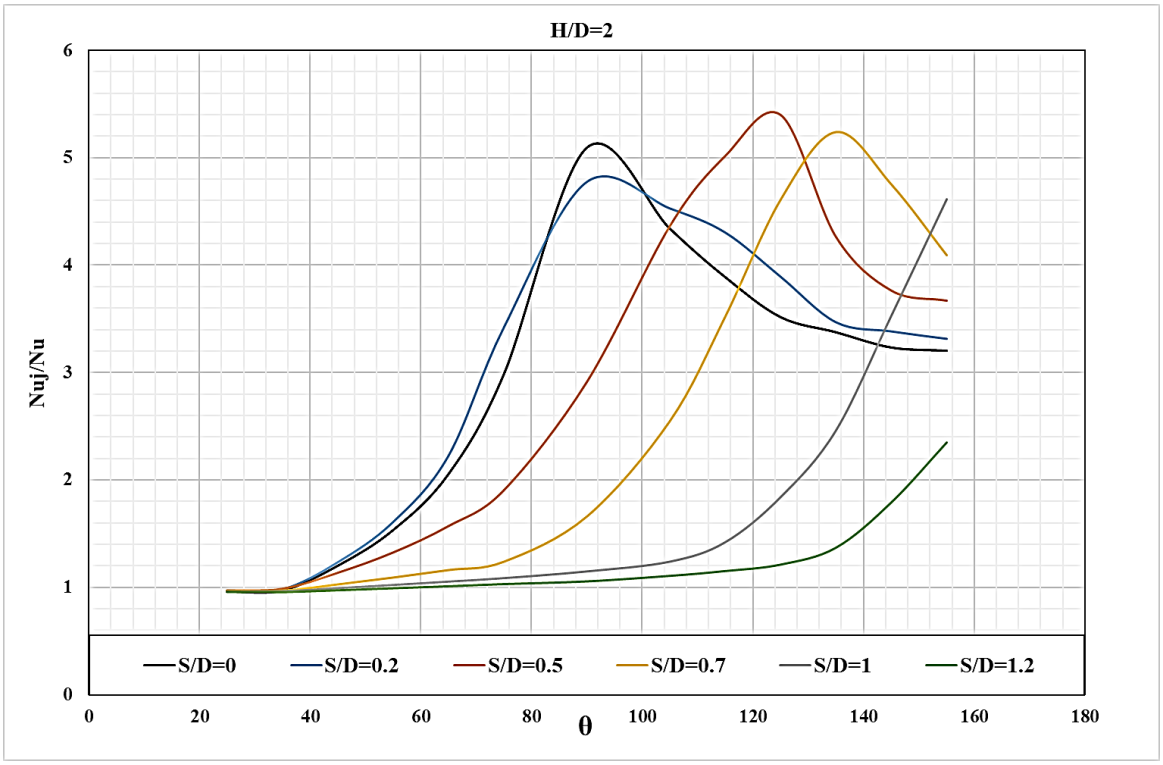

Figure 4 $\overline{Nu_j}/\overline{Nu}$ **vs (θ) at H/D=2 and different jet positions (S/D).**

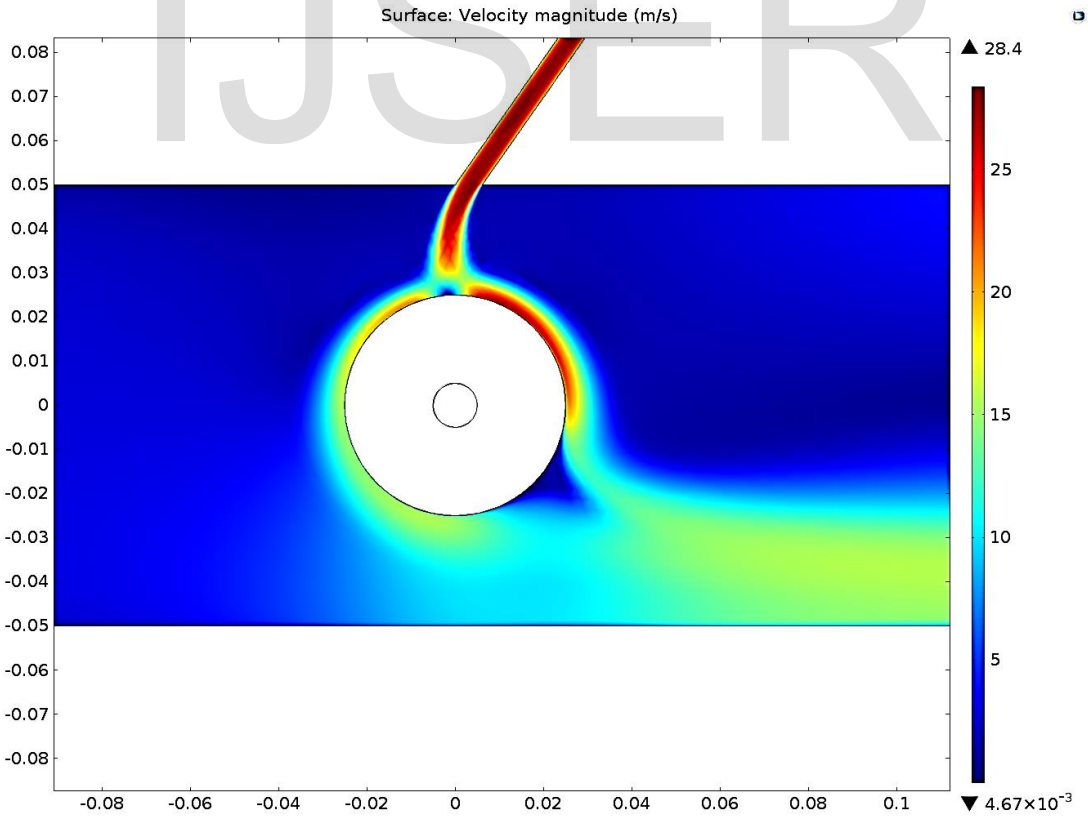

Figure 5 The velocity field for H/D=2, S/D=0.5, and θ =125°.

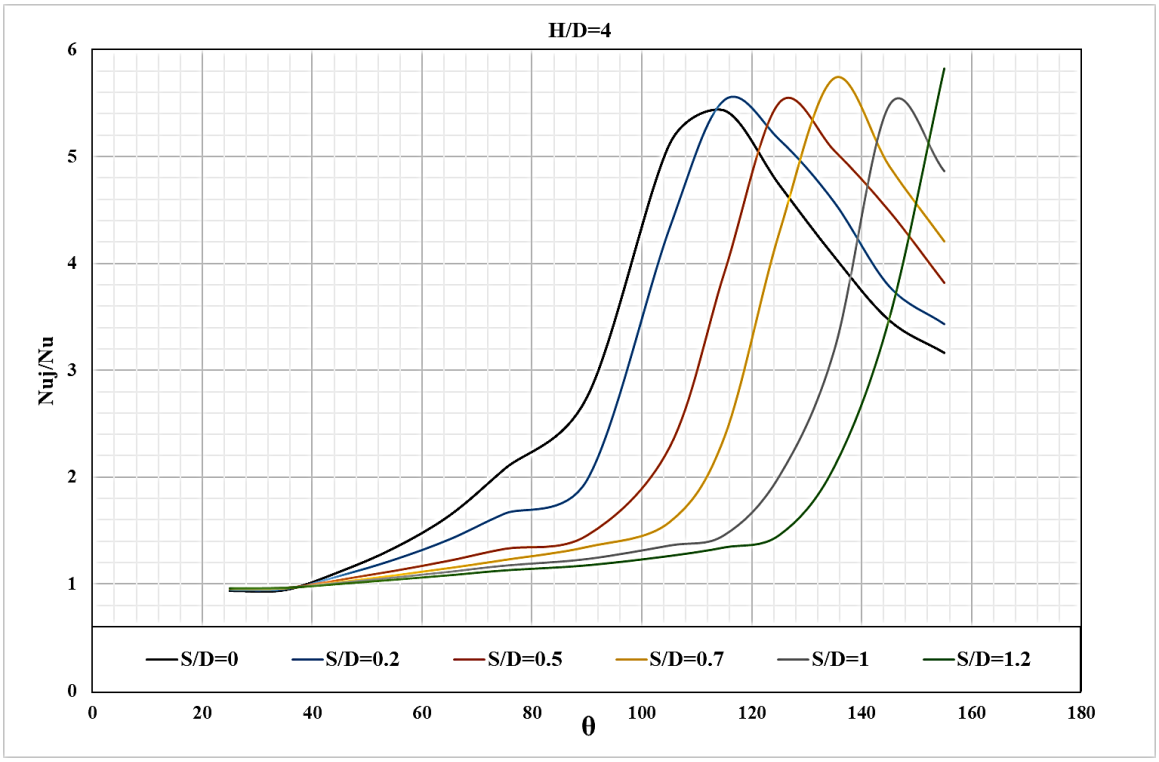

Figure 6 $\overline{Nu_j}/\overline{Nu}$ vs (θ) at H/D=4 and different jet positions (S/D).

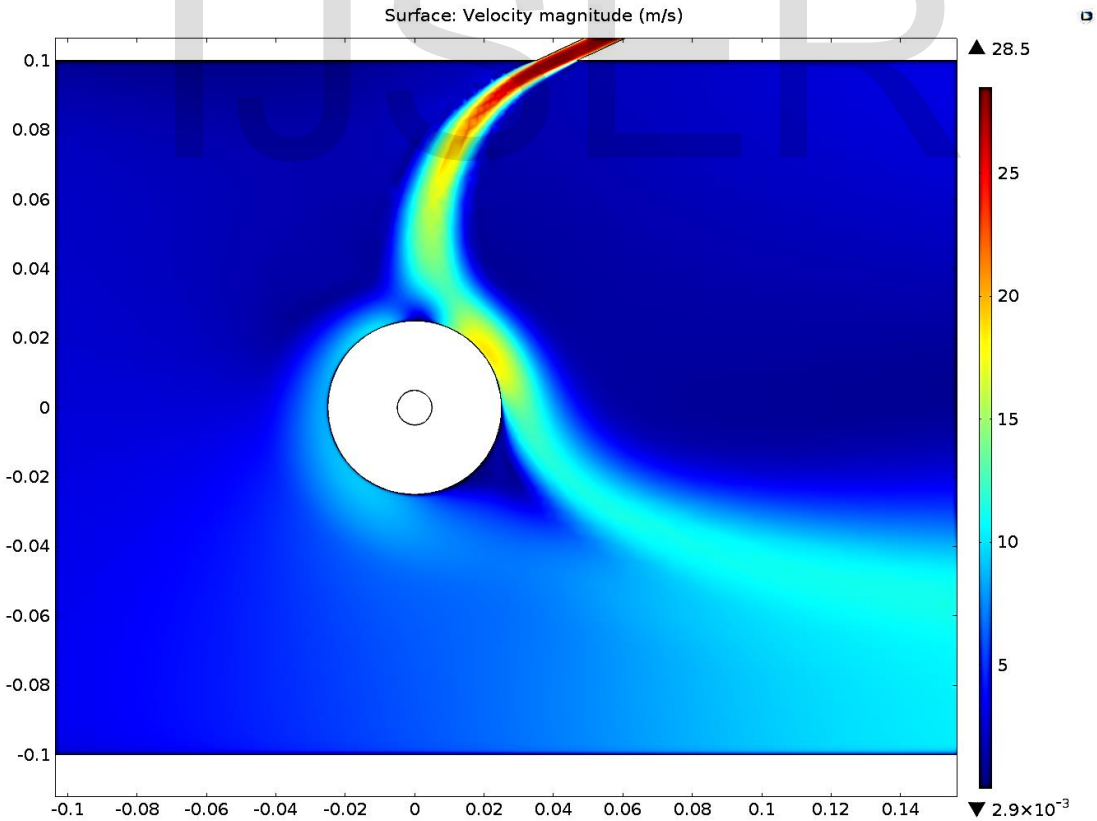

Figure 7 The velocity field for H/D=4, S/D=1.2, and θ =155°.

Figure 9 shows the velocity field for H/D = 4, S/D = 1.2, and θ = 155°. Although the velocity ratio of the crossflow to the jet is kept constant at 1:16, the effective momentum flux did not hit the surface of the cylinder at 90°. Almost all the jet flow passed downstream around the cylinder however the boundary layer suppression is good enough to increase Nusselt number ratio $\overline{Nu}_j/\overline{Nu}$ to 5.8.

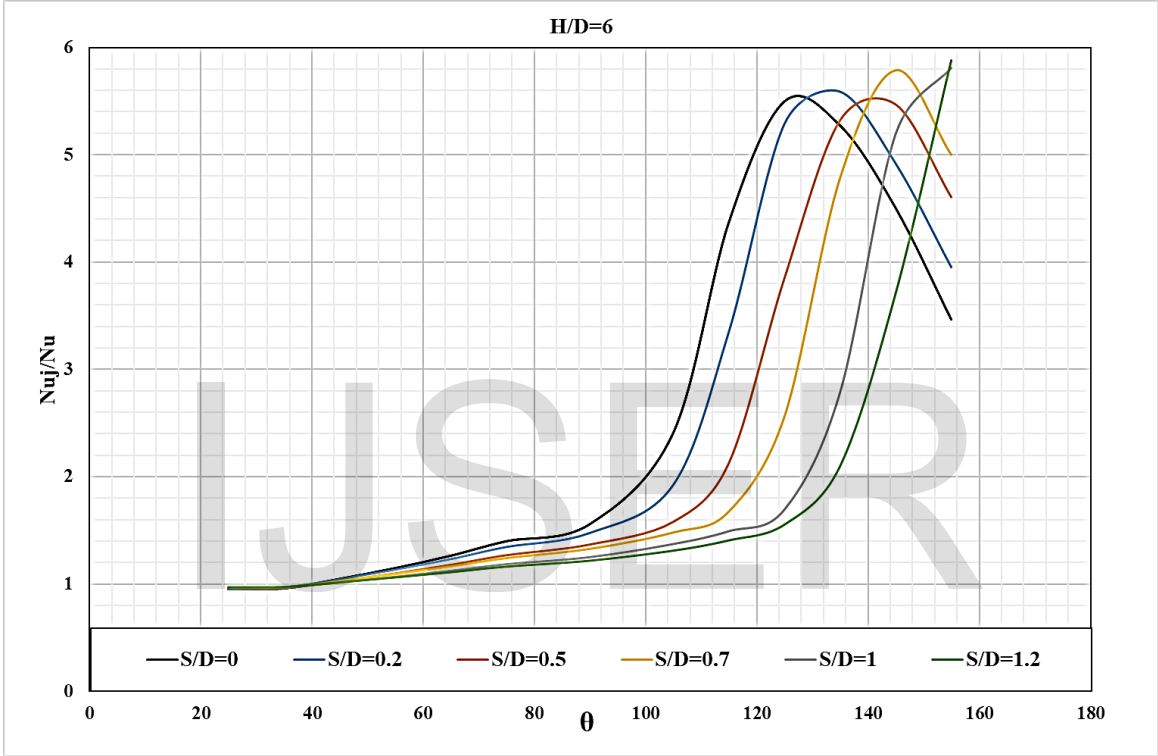

Figure 8 $\overline{Nu_j}/\overline{Nu}$ vs (θ) at H/D=6 and different jet positions (S/D).

So similar trends to that of H/D = 2 are observed except the peaks shift to higher jet angles. The decay of these peaks is attributed to the inability of the jet momentum to completely reach the cylinder surface and thus the suppression of the boundary layer is partial. At S/D = 1.2 however, the increase in $\overline{Nu}_j/\overline{Nu}$ reaches 5.8 at θ = 155° the decay is not visible though at this condition because the jet angle is limited to 155° in all experiments.

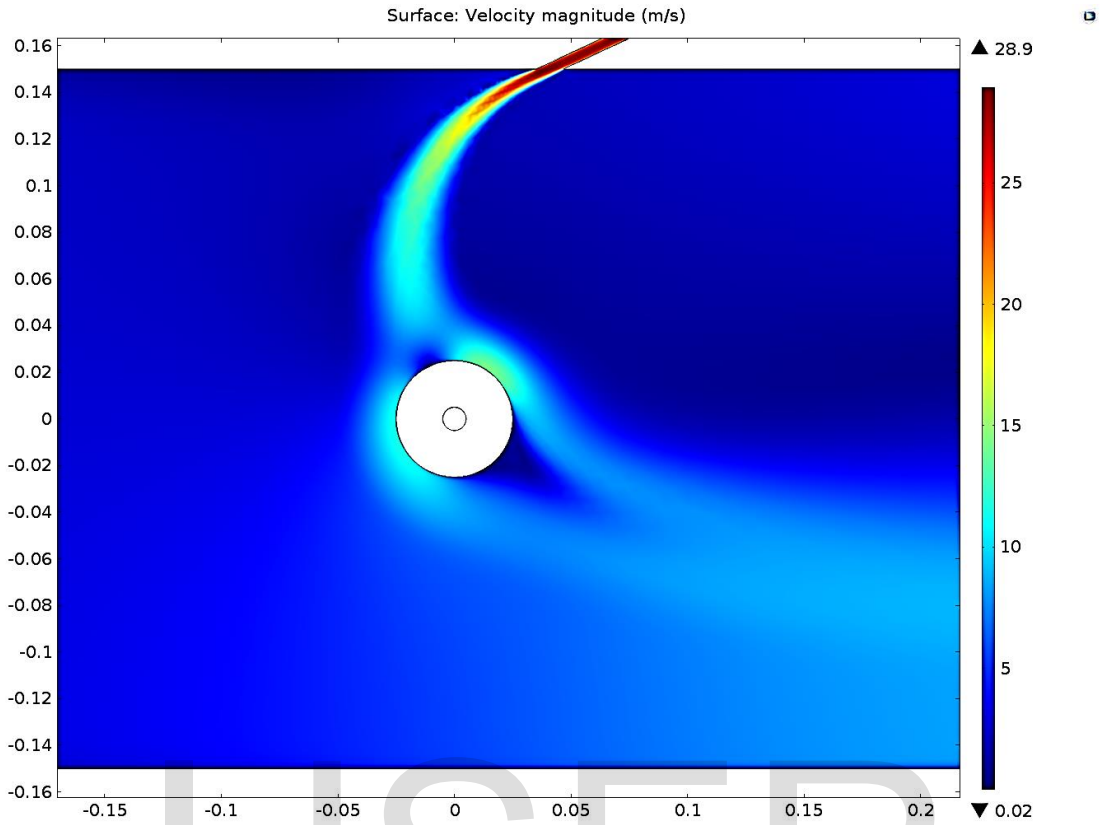

Figure 9 The velocity field for H/D=6, S/D=1.2, and θ =155º

Figure 10 shows the relationship between $\overline{Nu_j}/\overline{Nu}$ and the jet inclination angle (θ) at H/D = 6 and different jet positions. Similar to the characteristics at H/D = 2 and 4, Nusselt number ratio $\overline{Nu_j}/\overline{Nu}$ reaches 5.8. The maximum enhancement however is obtained in a narrower range of θ from 125° to 155°.

Figure 11 shows the velocity field for H/D=6, S/D=1.2, and θ=155°. Although the momentum of the jet splits upstream and downstream its intensity decreases as H/D increases to 6.

Figure 12 shows the relationship between $\overline{Nu_j}/\overline{Nu}$ and the jet inclination angle (θ) at H/D = 8 and different jet positions. Similar to the characteristics at H/D = 2 4 and 6, Nusselt number ratio $\overline{Nu_j}/\overline{Nu}$ reaches 5.6. The maximum enhancement however is obtained in a narrower range of θ from 135° to 145°.

Figure 13 shows the velocity field for H/D = 8, S/D =0.5, and θ = 145°. Although the momentum of the jet splits upstream and downstream its intensity further decreases as H/D increases to 8.

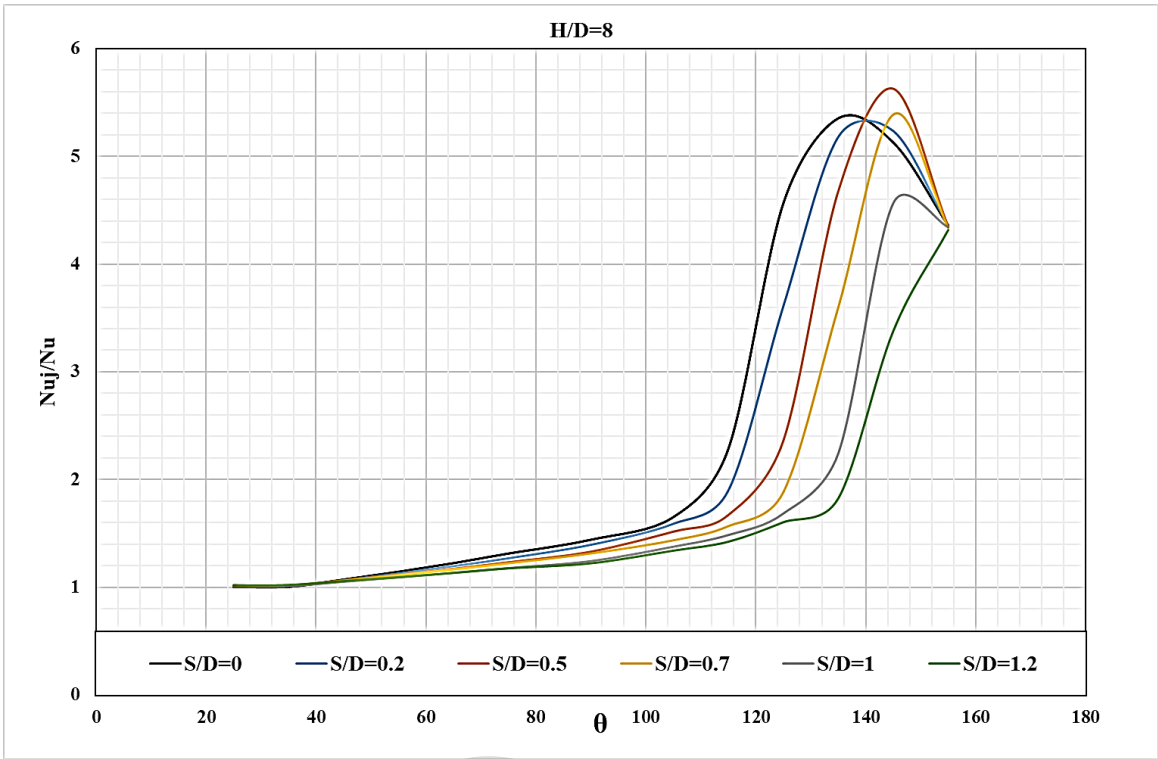

Figure 10 $\overline{Nu_j}/\overline{Nu}$ **vs (θ) at H/D=8 and different jet positions (S/D).**

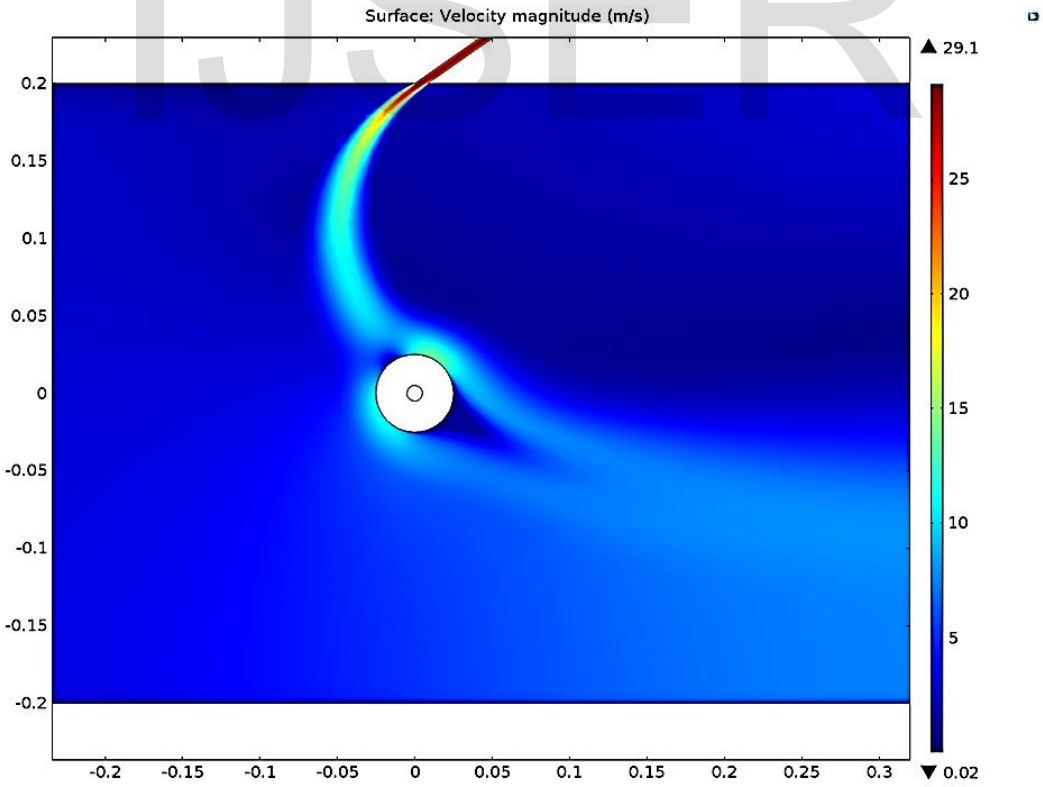

Figure 11 The velocity field for H/D=8, S/D=0.5, and θ =145º

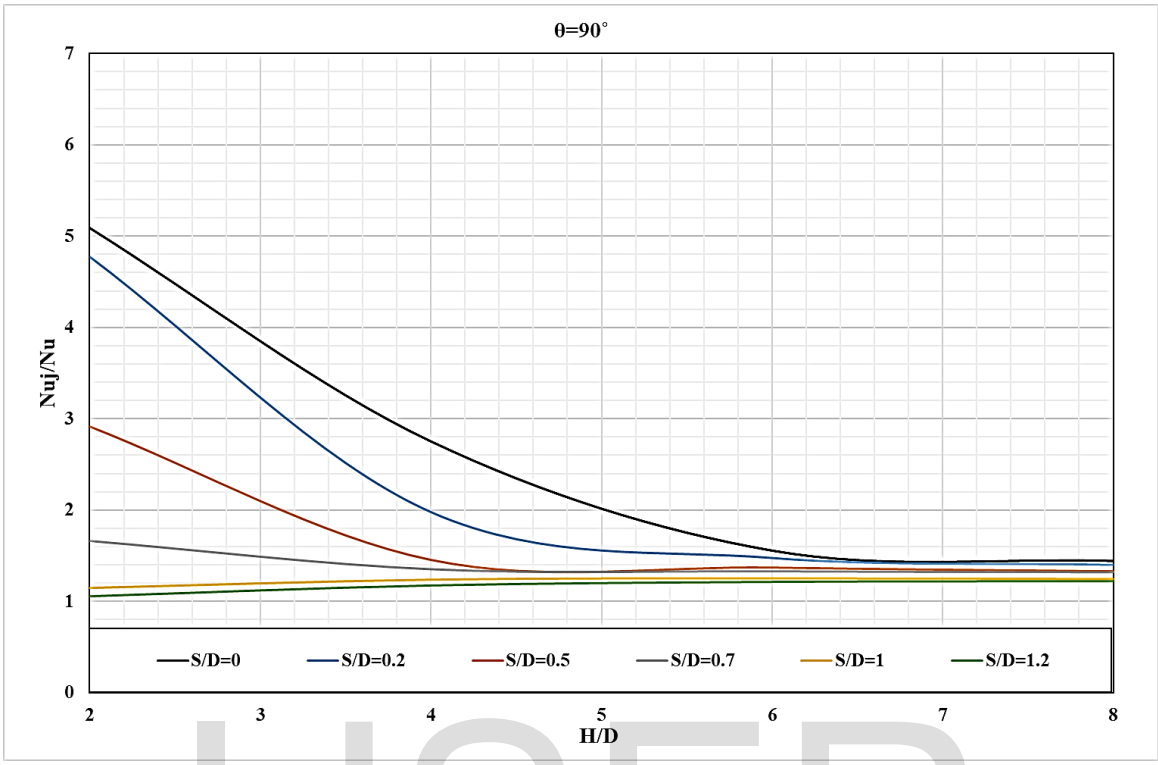

Figure 12 $\overline{Nu_j}/\overline{Nu}$ vs H/D at θ = 90º and different jet positions (S/D).

Figure 14 shows the relationship between $\overline{Nu_j}/\overline{Nu}$ and H/D at jet angle θ = 90º and different jet positions. The maximum enhancement of Nusselt number ratio $\overline{Nu_j}/\overline{Nu}$ is obtained at H/D = 2 where it reaches around 5 at S/D = 0. This is attributed to the significance of the jet momentum that reaches the cylinder surface where it is the best at the minimum value of H/D = 2 and where the jet is released the earliest downstream at S/D = 0. As H/D increases the enhancement in Nusselt number ratio $\overline{Nu_j}/\overline{Nu}$ starts to decay down to 1.2 - 1.4 for all jet positions S/D. $\overline{Nu_j}/\overline{Nu}$ reaches a constant value at H/D = 6.5.

For all H/D at jet positions S/D = 1 and 2, the enhancement in Nusselt number is anticipated to be zero, that is Nusselt number ratio $\overline{Nu_j}/\overline{Nu}$ is 1, however, there is a little enhancement in $\overline{Nu_j}/\overline{Nu}$ up to 1.2. This is attributed to the higher turbulence generated downstream by the introduction of the jet which affected the heat transfer mechanism positively by increasing the average Nusselt number and the ratio $\overline{Nu_j}/\overline{Nu}$ consequently. **Figure 15** shows the velocity field in the computational domain for θ = 90º, H/D = 2, and S/D of 0, 0.2, 0.5, and 0.7.

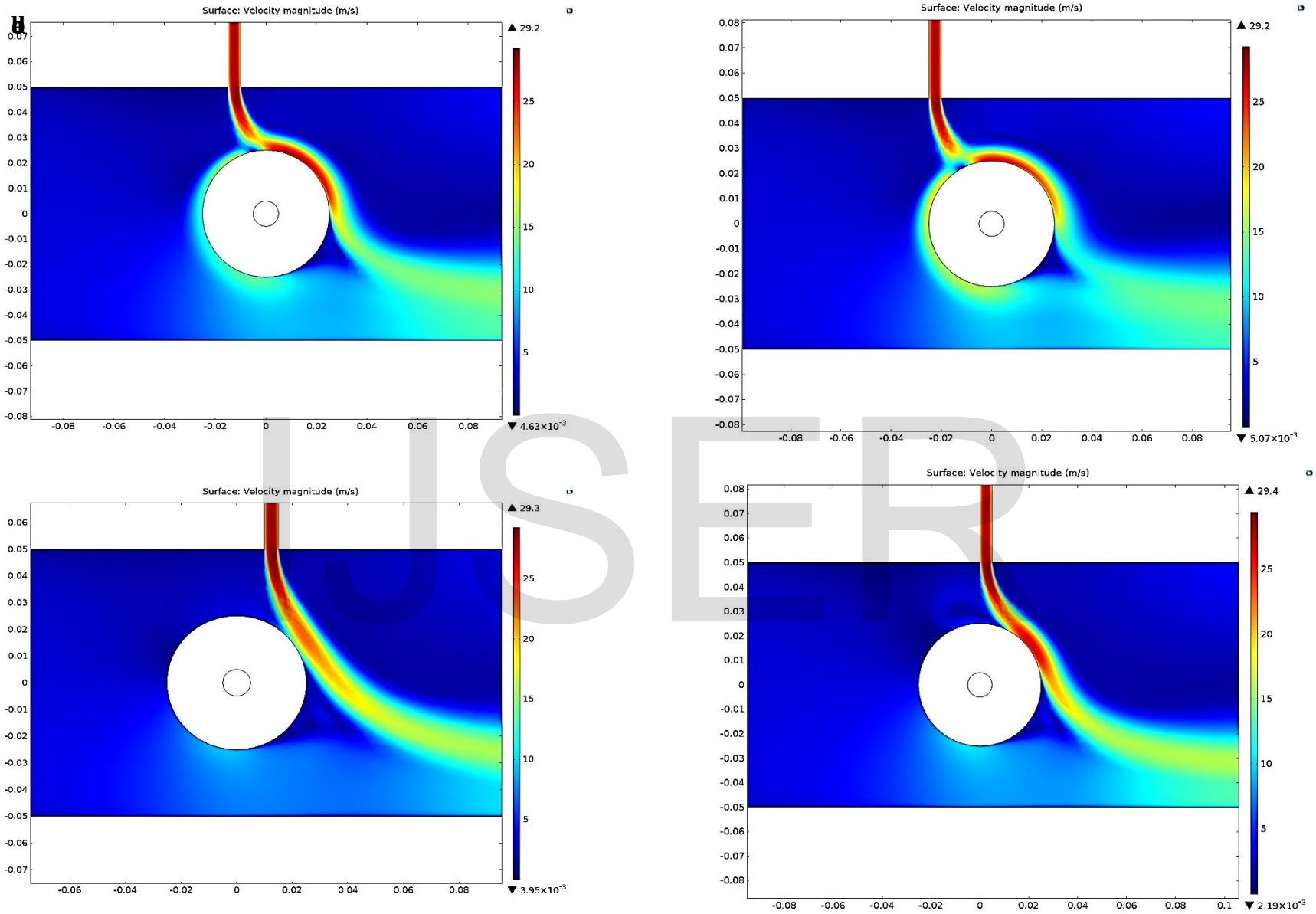

Figure 13 The velocity field at θ = 90º and H/D = 2: a) S/D=0, b) S/D=0.2, c) S/D=0.5, and d) S/D=0.7.

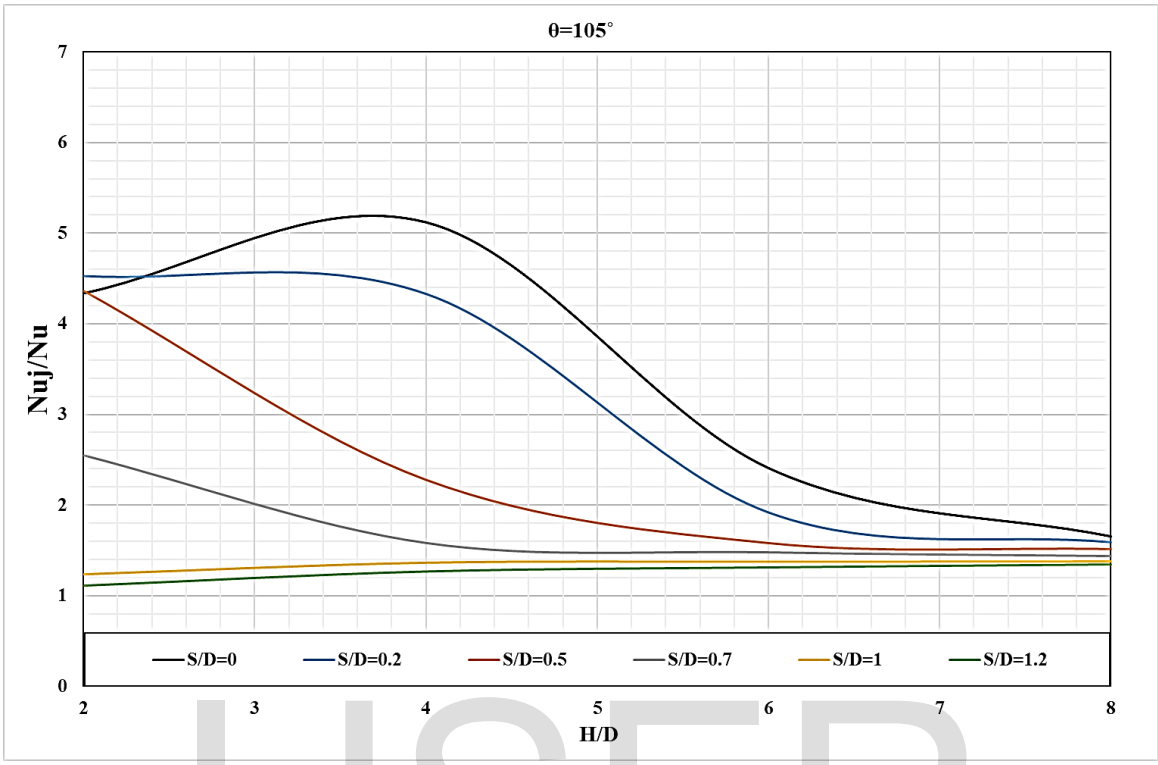

Figure 14 $\overline{Nu_J}/\overline{Nu}$ vs H/D at θ = 105º and different jet positions (S/D).

Figure 16 shows the relationship between $\overline{Nu_J}/\overline{Nu}$ and H/D at jet angle θ = 105º and different jet positions. The maximum enhancement of Nusselt number ratio $\overline{Nu_J}/\overline{Nu}$ is obtained at H/D = 3.7 where it reaches around 5.2 at S/D = 0. The maximum enhancement has shifted from H/D = 2 at θ = 90º to H/D = 3.7 at θ = 105º because the obtuse angle of the jet introduces jet momentum component in the upstream direction thus allowing the jet to reach the surface of the cylinder at higher distances H/D. This effect is noticeable for S/D = 0 and 0.2. At distances higher than 0.2 though this effect diminishes due to the inability of the jet momentum to reach the cylinder surface.

The enhancement in Nusselt number ratio $\overline{Nu_J}/\overline{Nu}$ starts to decay down to 1.2 - 1.6 for all jet positions S/D. The limit of this range increased from the case where θ = 90º due to the higher turbulence intensity generated in the wake of the cylinder downstream. **Figure 17** shows the velocity field in the computational domain for θ = 105º, H/D = 2 and 4, and S/D of 0, 0.2, 0.5, and 0.7.

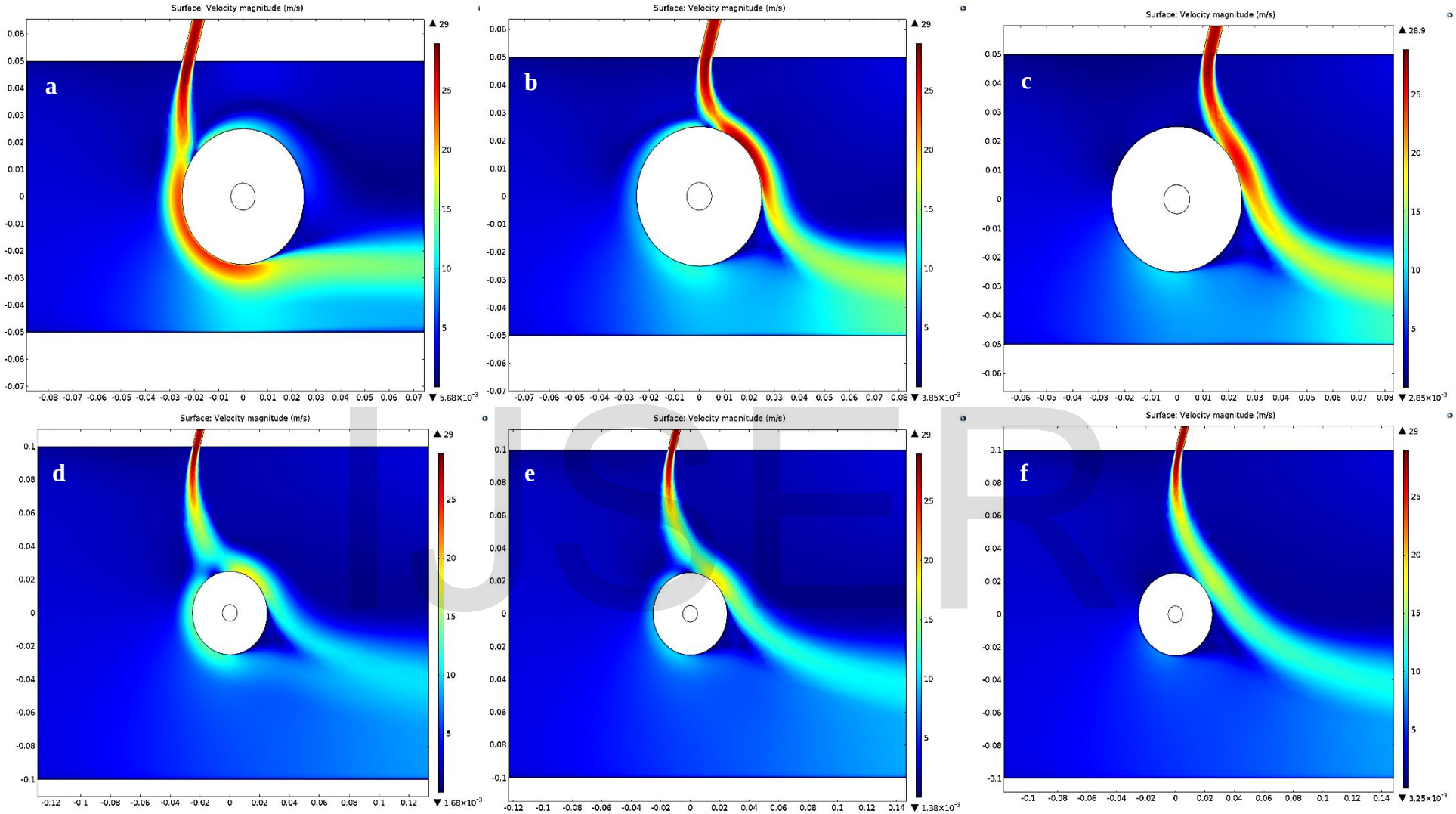

Figure 15 The velocity field at θ =105º: a) S/D = 0, H/D = 2 - b) S/D = 0.5, H/D = 2 - c) S/D = 0.7, H/D = 2 - d) S/D = 0, H/D = 4 - e) S/D = 0.2, H/D = 4 and f) S/D = 0.5, H/D = 4.

4. CONCLUSION

A two-dimensional numerical study was performed to show the effect of applying secondary jet flow on a circular cylinder that is cooled by a traditional crossflow of air. The velocity ratio of the air jet to the crossflow is kept constant at 16 for all cases under study. Different jet configuration was generated and tested to study the effect of the jet angle (θ), dimensionless jet spacing (S/D), and dimensionless duct height (H/D) on the heat transfer performance. Results show that the maximum enhancement in Nusselt number is 5.8 times that of the case with no jet where the mass flow rate of the two cases is kept the same. The best enhancement in Nusselt number can be achieved at all angles but different spacing at (H/D) = 2. The momentum of the jet contributed dramatically to enhancing the heat transfer mechanism by suppressing the boundary layer however a wider range of the tested parameters is advised in future work to get a better idea about this mechanism of enhancement.

REFERENCES

1. Singh, D., B. Premachandran, and S. Kohli, *Double circular air jet impingement cooling of a heated circular cylinder.* International Journal of Heat and Mass Transfer, 2017. **109**: p. 619-646.

2. Singh, D., B. Premachandran, and S. Kohli, *Circular air jet impingement cooling of a circular cylinder with flow confinement.* International Journal of Heat and Mass Transfer, 2015. **91**: p. 969-989.

3. Singh, D., B. Premachandran, and S. Kohli, *Experimental and numerical investigation of jet impingement cooling of a circular cylinder.* International Journal of Heat and Mass Transfer, 2013. **60**: p. 672-688.

4. Bharti, R.P., R.P. Chhabra, and V. Eswaran, *A numerical study of the steady forced convection heat transfer from an unconfined circular cylinder.* Heat and Mass Transfer, 2006. **43**(7): p. 639-648.

5. Mettu, S., N. Verma, and R.P. Chhabra, *Momentum and heat transfer from an asymmetrically confined circular cylinder in a plane channel.* Heat and Mass Transfer, 2006. **42**(11): p. 1037-1048.

6. Khan, W.A., J.R. Culham, and M.M. Yovanovich, *Fluid Flow Around and Heat Transfer From an Infinite Circular Cylinder.* Journal of Heat Transfer, 2005. **127**(7): p. 785.

7. Khan, W.A., J.R. Culham, and M.M. Yovanovich, *Fluid Flow and Heat Transfer from a Cylinder between Parallel Planes.* Thermophysics and Heat transfer, 2004. **18**.

8. Sanitjai, S. and R.J. Goldstein, *Forced convection heat transfer from a circular cylinder in crossflow to air and liquids.* International Journal of Heat and Mass Transfer, 2004. **47**(22): p. 4795-4805.

9. Tawfek, A.A., *Heat Transfer due to a round Jet impinging normal to a cicular cylinder*>. Heat and Mass Transfer, 1999. **35**: p. 7.

10. Tawfek, A.A., *Heat Transfer studies of the oblique impingement of round jets upon a curved surface.* Heat and Mass Transfer, 2002. **38**: p. 9.

11. R.M. Fand, *Heat transfer by forced convection from a cylinder to water in crossflow*, Int. J. Heat Mass Transfer 8 (1965) 995–1010. [7] H.C. Perkins, G. L.